Journal of Low Temperature Physics, Vol. 29, Nos. 1/2, 1977

The Behavior of the ^{4}He Viscosity Near the Superfluid Transition*

L. Bruschi, G. Mazzi, M. Santini, and G. Torzo

Istituto di Fisica, Università di Padova, Gruppo Nazionale Struttura della Materia, Padova, Italy

(Received April 26, 1977)

Measurements of the shear viscosity at saturated vapor pressure through the lambda transition indicate a singular behavior of the form $|1-(\eta/\eta_\lambda)| = A\varepsilon^x$, *(where* $\varepsilon = |1-(T/T_\lambda)|$, *with equal values for the critical exponent on both sides of the transition.*

1. INTRODUCTION

Results of measurements of the viscosity η of liquid ^{4}He near the superfluid transition have been already reported by us.[1] The motivation of that experiment and also of the present one was to reach a conclusion on the behavior of η at the λ transition. From the earlier data near T_λ,[2] we know that η is continuous at T_λ. These data, analyzed and summarized by Ahlers,[3] show also that η varies rapidly with T, and that it is likely to be singular at T_λ. All the available results were represented by the function

$$|1-(\eta/\eta_\lambda)| = A\varepsilon^x \tag{1}$$

where $\varepsilon = |1-(T/T_\lambda)|$. Both the strength A and the critical index x are different on either side of the transition, $A = 5.19$ and $x = 0.85$ for $T < T_\lambda$, and $A = 1.82$ and $x = 0.75$ for $T > T_\lambda$. The data are well fitted by the function (1) for $10^{-4} \leq \varepsilon \leq 10^{-2}$, even if the behavior of η at smaller ε is not clear from these earlier results.

Subsequent measurements in ^{3}He–^{4}He mixtures,[4] however, show that both η and $d\eta/dT$ are continuous at T_λ. Extrapolation at zero ^{3}He concentration led the authors to conclude that η is regular at the transition.

Some questions were raised at that point. Assuming that η is continuous at T_λ, what is the real behavior of the temperature derivative? We are also interested in the temperature dependence of η—to know, as an

*Work sponsored by Consiglio Nazionale delle Ricerche, Rome (Italy).

example, whether or not the simple power law (1) is really followed at the smallest ε. If this is the case, does the critical index x take on equal values on both sides of the transition and at different pressures, as expected in a genuine critical behavior?

To answer these questions, we undertook experiments with the vibrating wire technique,[5] using it in a greatly improved version developed in our laboratory.[6] In a first set of experiments we did measurements only for $T < T_\lambda$,[1] following the behavior of viscosity down to $\varepsilon \simeq 10^{-5}$. We found that the power law (1) is well obeyed, with numerical values for A and x which are consistent with Ahlers' analysis.[3]

Almost at the same time, Biskeborn and Guernsey (BG) published the results of their measurements taken with an oscillating hollow cylinder on both sides of the transition.[7] These authors found that a fit of their data to Eq. (1) yields $x = 0.80 \pm 0.05$ for $T > T_\lambda$ and $x = 0.65 \pm 0.03$ for $T < T_\lambda$. Moreover, for $T < T_\lambda$ and $\varepsilon \geq 4 \times 10^{-4}$ the data deviate from this fit, approaching the fit given by Ahlers[3] to the data of earlier experiments.[2] The results of the BG experiments below T_λ and ours were therefore in disagreement.

This discrepancy drove us to improve once more our technique, and to check the effects of some approximations involved in the calculation of the viscosity. At the same time we set up a new cryogenic apparatus suitable for measurements at $T > T_\lambda$. As a result of our work we found that the power law (1) is well followed for $10^{-5} \lesssim \varepsilon \lesssim 10^{-2}$, and that the critical exponent x takes on the same value, within the experimental errors, on both sides of the transition. Our results for $T > T_\lambda$ are in agreement with those of BG, but the discrepancy still remains at $T > T_\lambda$.

The results of our work are presented in this paper. Details on our technique and its application to liquid helium can be found in previous papers.[1,6] In Section 2 we describe some important features of the relative method used in the present work and the details on the experimental apparatus. Experimental results and data analysis are reported in Section 3, while a discussion and conclusion can be found in Section 4.

2. EXPERIMENTAL METHOD AND APPARATUS

2.1. The Method of Measurement

The measurements of viscosity presented in this paper were performed with the vibrating wire technique.[5] We used a tungsten wire of 5×10^{-3} cm diameter stretched in a constant magnetic field B. The vibration of the wire is detected by the voltage induced in the wire circuit. The viscosity η of the liquid helium in which the wire is vibrating can be measured starting with the

measure of the resonance width $\Delta\nu$.[6] Calculations are then made with the aid of the Stokes theory for the oscillating cylinder.[8]

In the present experiments, however, we measured η with a relative method,[6] which is more convenient for small viscosity changes. The wire is driven to vibrate exactly at its resonant frequency f_0 by a sine wave voltage of constant amplitude V_D. This voltage is applied to the wire through a resistance R, much greater than the wire resistance. We therefore drive the wire by a sine current of constant amplitude $i_0 = V_D/R$. The induced voltage v_0 at resonance is given by

$$v_0 = Di_0/\rho f_0 k' = DV_D/\rho f_0 k' R \tag{2}$$

D is a constant and depends upon the magnetic field B and the length and radius of the wire, f_0 is the resonant frequency, and ρ is the total density of liquid helium if we are measuring in He I, the normal density if we are measuring in He II. In (2), k' is a frequency-dependent viscous coefficient. Its value is given by the Stokes theory as a function of the parameter

$$m = (a/2)(2\pi f\rho/\eta)^{1/2} = (a/2\lambda) \tag{3}$$

where $\lambda = (\eta/2\pi f\rho)^{1/2}$ is the viscous penetration depth. At a frequency $f \simeq 4000$ Hz, $m \simeq 15$ in the lambda region. It can be shown[1] that in this situation

$$\eta = \frac{\pi a^2 D^2}{R^2 C(k')} \frac{V_D^2}{\rho f_0 v_0^2} \tag{4}$$

where $C(k') = 2 + k' + 2(1+k')^{1/2}$. This parameter depends only weakly upon temperature through viscosity and density. Because of the narrow temperature range, we can assume it to be a constant. The induced voltage v_0 is amplified through a high-stability gain amplifier and detected with a phase sensitive detector. As a result, we measure an output voltage $V_0 = Gv_0$. With this position and taking $C(k') = \text{const}$ we have from (4)

$$\eta = \frac{EG^2}{\rho f_0 (V_0/V_D)^2} \tag{5}$$

where E summarizes the constants of relation (4). As the viscosity changes to be detected are very small, the amplitude V_D of the driving voltage must be stable. To avoid spurious results due to a possible drift in V_D it is better to measure the ratio $v = V_0/V_D$ between the output and the driving voltage, rather than V_0 itself. For this purpose we have introduced some modifications in our electronics, which enables us to measure the ratio v. The gain G is usually constant over the time interval of interest and we can therefore

write, from (5),

$$\eta = H/\rho f_0 v^2 \tag{6}$$

where H is the new appropriate constant. The relationship (6) defines our viscosity in arbitrary units as a function of the measured quantities ρ, f_0, and v.

What about the error introduced by the assumption $C(k') = \text{const}$? We are mainly interested in the dependence of the reduced viscosity $\eta^* = |1-(\eta/\eta_\lambda)|$ on the reduced temperature $\varepsilon = |1-(T/T_\lambda)|$. The coefficient k' is about 0.1 in our experiments, and its relative changes are smaller than 1% between $\varepsilon = 10^{-2}$ and $\varepsilon = 10^{-6}$ for $T < T_\lambda$. The relative changes of $C(k')$ are therefore smaller than 5×10^{-4} and the approximation seems to be good.

It is to be noted, however, that the reduced viscosity η^* also becomes very small as $\varepsilon \to 0$. If we investigate this point more carefully, we find that the approximation $C(k') = \text{const}$ is a very good one for the He I region, but it introduces a final error of about 1% on the critical exponent x for $T < T_\lambda$. We retain the approximation contained in the definition (6) as being good enough for our purposes. It is to be stressed, however, that the problem just discussed, and treated in detail in Appendix A, can be a clear example showing that approximations must be handled very carefully.

The internal dissipation of the wire is very small with respect to the viscosity dissipation. The quality factor Q_0 in vacuum is in fact about 4×10^5 at helium temperatures. It is about 400 times greater than the quality factor Q measured with liquid helium. Therefore the internal dissipation of the wire only results in a negligible correction to the measurements. If we completely neglect it, we introduce a final error of about 0.1% on the critical exponent x, as shown in Appendix B.

2.2. The Measuring Cell

A schematic view of the cryogenic arrangement is given in Fig. 1. A small bar of lavite supporting the wire is placed inside a copper cell together with the permanent magnet. The wire lies in a horizontal position, and the magnetic field is aligned in such a way that only one of the two vibration modes is essentially excited.[6]

The main thermometer is a germanium resistance thermometer (Leico Industries, Model 3L). It is placed inside the cell in direct contact with the liquid. Two auxiliary Allen Bradley 100 Ω resistors R_1 and R_2 are submerged in the liquid, the first at the bottom of the cell, the other at the wire level. These resistors form the arms of a bridge, as shown in Fig. 2, and are used to detect a possible thermal gradient in He I and the occurrence of the λ transition.

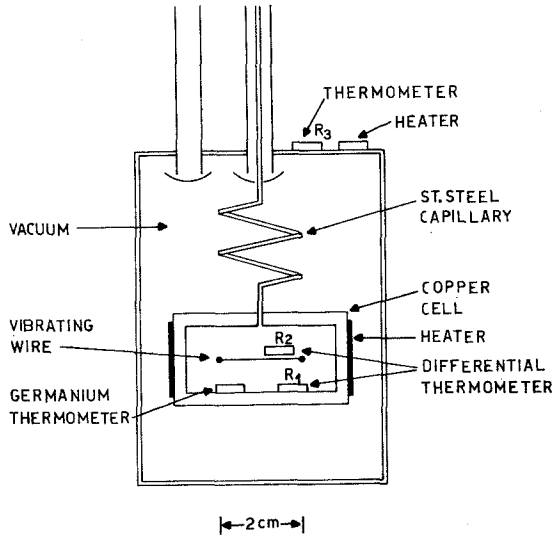

Fig. 1. Schematic view of the cryogenic apparatus. In the most recent experiments the germanium thermometer was placed at the wire level.

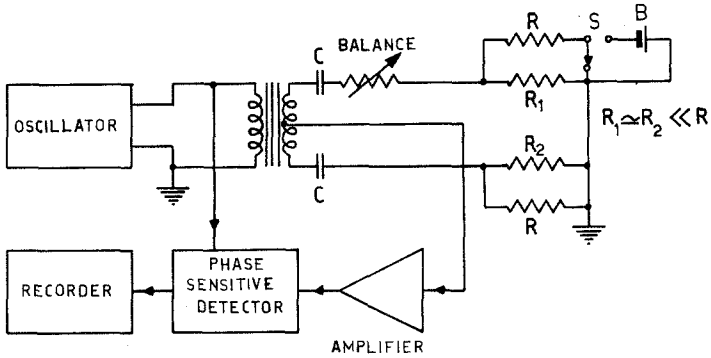

Fig. 2. Block diagram of the differential thermometer bridge. With connections as shown the dissipations on R_1 and R_2 are the same, and the circuit is used to detect thermal gradients. To detect the λ transition the position of S is changed, allowing an extra dissipation on R_1 through the battery B. Not shown is an analogous detail for R_2.

The measuring cell is suspended inside a brass vacuum chamber immersed in the main bath, whose temperature is measured and regulated using a third carbon resistor R_3 fixed on the outside wall of the chamber. The filling capillary is surrounded by a vacuum space and it is moderately heated to prevent condensation of liquid in the capillary itself, the main bath usually being kept colder than the cell. This condensation produces an appreciable thermal gradient within the liquid for $T > T_\lambda$. Moreover, it causes a noisy thermal contact between the cell and the main bath, which hinders us from obtaining a good thermoregulation.

2.3. Temperature Measurement and Control

The bridge and electronics used in our previous experiments were greatly improved, together with thermoregulation at room temperature of the reference resistor R_N. To check the stability of the whole circuit, we measured over a long time the resistance of a high-stability resistor R thermoregulated at room temperature. The value of this resistance was about 400 kΩ, which is the value of our germanium resistance at $T \simeq T_\lambda$. The bridge unbalance changed slowly, as if a relative change $\Delta R/R = \pm 5 \times 10^{-6}$ over 20 h was present. This figure for unbalance drift includes both resistance changes ΔR and ΔR_N and electronics drift. If related to a real experiment in liquid helium, it corresponds to a spurious temperature change of $\pm 2.5 \times 10^{-6}$ K over 20 h.

The main bath was thermoregulated to within 10^{-4} K at $T \simeq (T_\lambda - 5 \times 10^{-2}\,\mathrm{K})$ with the aid of a pressostat and a standard thermoregulator. The temperature of the cell was stabilized through a heater directly wound on its outside and driven by the output stage of the germanium thermometer electronics. As a result of electronics and cryogenic improvements, it was possible to keep and measure the temperature to within $\pm 1 \times 10^{-6}$ K, with a dissipation on the main thermometer never greater than 5×10^{-9} W.

2.4. Determination of the λ Point

The λ transition was detected through the change of thermal conductivity that occurs at T_λ. The jump was monitored by means of the two carbon resistors R_1 and R_2. Because they were chosen to have a very small difference in resistance, the bridge remained well balanced when the temperature was changed. The small power dissipation due to ac currents is the same for R_1 and R_2 and therefore the bridge does not feel the T_λ crossing. With our arrangement, however, we can increase the power dissipation in R_1 or R_2 by means of a small dc current as shown in Fig. 2. In this condition the bridge unbalance must change when crossing T_λ, because of the different self-heating changes in the two thermometers.

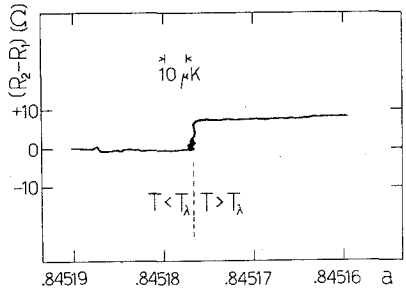

Fig. 3. A record of the λ-point crossing obtained on an XY recorder. X axis: calibrated dc output of the main thermometer phase-sensitive detector. Y axis: resistance differences between carbon resistors R_1 and R_2.

The outputs of the main and the auxiliary bridges are connected to an XY recorder, and the cell temperature is released to drift slowly across the λ point. One of the records obtained crossing the λ point is shown in Fig. 3. By means of these records we measure the value R_λ of the main thermometer at T_λ. This one was calibrated during the same run against the vapor pressure of the cell bath, measured by a mercury manometer and a high-precision cathetometer. The T_λ value measured in this way was $T_\lambda = 2.1720 \pm 0.0001$ K, in very good agreement with the commonly accepted value.

The calibration of the main thermometer was performed only in the first run of the experiments here described. For temperatures between 2.0 and 2.4 K we found an accurate linear relation between the temperature T and the value a of the ratio transformer that balances the bridge, $T = A - Ba$. We are interested only in the value of $T - T_\lambda$ that is given by $T - T_\lambda = -B(a - a_\lambda)$, and we assumed the calibration of the first run to be valid for the other runs, too. We have found indeed only a small shift in a_λ upon thermal cycling and aging. Values of a_λ measured in various runs over one month are shown in Fig. 4. The maximum change with respect to the value a_λ

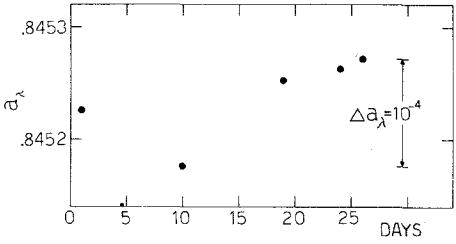

Fig. 4. Value a_λ of the ratio transformer dial number a at which the germanium bridge is balanced at T_λ. Results of various runs. The shift comprises changes in germanium resistance, reference resistance, and electronics.

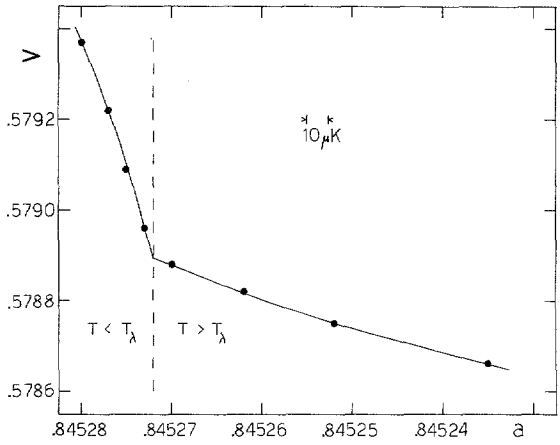

Fig. 5. The output/input voltage ratio v measured at various equilibrium temperatures near the transition. From plots like these we derive the values $M_{\lambda 0}$ and $a_{\lambda 0}$ used in the first step of the best-fit calculation.

of the first run corresponds to a possible shift in T_λ of only 2×10^{-4} K. This result allows us to avoid calibration run by run.

The λ transition also can be detected by the wire signal itself. In fact, the wire signal changes rapidly with temperature at $T<T_\lambda$ and slowly for $T>T_\lambda$ (see Fig. 5). As the change of the slope dv/dT is very sharp at the transition, we can use it to determine the value a_λ of the run under way. The values of a_λ measured with the two methods agree to within experimental errors, leading to a possible difference in T_λ of $\pm1\,\mu$K.

3. EXPERIMENTAL RESULTS

3.1. Experimental Conditions

3.1.1. Line Shape and Signals

The wire was positioned in a magnetic field of about 600 G produced by a small permanent magnet. Unless the magnetic field is perfectly aligned, two peaks will be found in the resonant region.[6] The separation s between the resonant frequencies amounts to about three linewidths in our case. Therefore the measurement of the linewidth $\Delta\nu$ and of the signal amplitude v of the main peak is affected by the contribution of the second peak. It is possible to show that if the ratio $R=v_2/v_1$ between the second and the main peak amplitudes is smaller than 0.1, the final error in the critical exponent can be neglected (see Appendix C).

No particular alignment was performed, mounting, however, the wire and the magnet as explained in Ref. 6. The resonance region was accurately scanned to detect the second peak at room temperature and at 4.2 K with a good vacuum in the cell. The peak ratio $R = v_2/v_1$ was estimated to be smaller than 0.05. This value was also confirmed by the symmetric positions of the side frequencies f_1 and f_2 with respect to the resonant frequency f_0, and by the measurement of the signal amplitude, which must be the same at f_1 and at f_2 for a pure resonant line. The wire was driven by a sine current of amplitude ranging between 15 and 150 μA rms. Two resonant frequencies were used, $f_0 \simeq 3000$ Hz and $f_0 \simeq 4500$ Hz, while the resonant signal v_0 was in the range between 1.3 and 13 μV rms. The mean power dissipated by the wire was therefore less than 2×10^{-9} Watt.

Power radiated by sound and compressibility effects can be neglected, as explained in previous papers.[1,6]

3.1.2. Impurity Effects

In the course of the present work we discovered a striking effect due to the presence of impurities. In the earlier runs we usually filled the cell with helium, passing the gas through a charcoal trap at 77 K, but without too much caution. The experimental situation was satisfactory. A casual change of the high-pressure helium cylinder produced a new and discouraging situation.

The major features of this impurity effect can be summarized as follows. (1) We have observed it only in cryogenic liquids (helium, nitrogen, etc.), but never in gases or in saturated vapors. (2) The linewidth $\Delta\nu$ is greater than expected (10–50% greater), and slowly increases with time. A stationary situation is reached after many hours. (3) The effect depends upon the oscillation amplitude y_0, in the sense that an increase in y_0 rapidly increases the linewidth to a new value $\Delta\nu_1$. After y_0 has been decreased back to the initial value, $\Delta\nu$ takes a value $\Delta\nu_2 \simeq \Delta\nu_1$. We have therefore a kind of hysteresis effect. After many trials and failures and all possible checks on the electronics, we realized that the effect was due to impurities, probably small oil particles, which can be present in high-pressure cylinders, or simply gaseous impurities. The effect was in fact more pronounced when we filled the cell without the use of the filtering trap. Our explanation is that impurities close to the wire can be attracted to it, probably by image electrostatic forces. Because the wire is very thin (50 μm), the relative increase in the effective diameter can be appreciable, causing a broadening of the linewidth. The effect is not relevant in gases and vapors, because their density is smaller than the liquid density. We have therefore fewer impurities, and probably they cannot float in the cell.

Using liquid nitrogen as a check liquid, we redesigned completely the traps and filtering setup until the effect disappeared. After this long trial we reached a satisfactory situation. The results reported in this paper were obviously taken in a clean situation. We have reported, however, the impurity effect in some detail, because it is likely to be found by other workers. If the linewidth is larger than expected and depends upon the oscillation amplitude with hysteresis effects, then the response of the vibrating wire and probably the viscosity itself are being affected by impurities. Because of the thinness of the wire, our viscometer is, in a sense, a rather delicate one. On the other hand, it shows by itself the presence of impurities.

3.1.3. Amplitude Effects

The Stokes theory of the oscillating cylinder is developed neglecting nonlinear terms in the Navier–Stokes equations. If we use this theory to calculate the viscosity coefficient, the linewidth or the resonant signal must be measured at very low vibration amplitudes. From order-of-magnitude arguments one gets the conditions $y_0 \ll a$, $y_0 \ll \lambda$, where y_0 is the vibration amplitude, a the wire radius, and λ the penetration depth. Because $\lambda < a$, the condition is $y_0 \ll \lambda$, which is a rather strong one. In fact $a = 2.5 \times 10^{-3}$ cm, and for $f = 4000$ Hz the penetration depth, which is practically constant in our temperature range, has the value $\lambda \simeq 8.6 \times 10^{-5}$ cm.

A more realistic condition can only be derived from experiments, measuring, for example, the linewidth $\Delta\nu$ as a function of y_0. If the impurity effect is absent, the measurement is quite easy, and we did it in He II. We found that the dependence of $\Delta\nu$ on y_0 is very weak indeed. Up to the maximum amplitude used in our measurements ($v_0 = 13\ \mu$V, $y_0/\lambda = 0.7$) the linewidth $\Delta\nu$ is practically constant. The results are in fact statistically distributed around the mean value $\Delta\nu_M$, within $\pm 5 \times 10^{-4} \Delta\nu_M$ (Fig. 6). These results show both the absence of the impurity effect and the high degree of reproducibility with our technique.

Analogous results have been obtained in liquid nitrogen ($\eta = 1.58 \times 10^{-3}$ P, $\rho = 0.808$ g/cm, and $\lambda = 2.8 \times 10^{-4}$ cm), using the same cell used for He II. Here also we have practically no amplitude dependence up to 42 μV (corresponding to an amplitude $y_0 = 0.7\lambda$). A broadening of 0.8% is obtained only at an induced voltage $v_0 = 100\ \mu$V ($y_0 = 1.66\lambda$). The situation is therefore much better than expected from a coarse order-of-magnitude calculation.

Our measurements were taken at constant driving voltage. The amplitude y_0 and the ratio y_0/λ are therefore weakly temperature dependent. On the whole range covered by our measurements the change of y_0/λ is about 4% for $T > T_\lambda$ and 12% for $T < T_\lambda$. If one has an error due to the finite

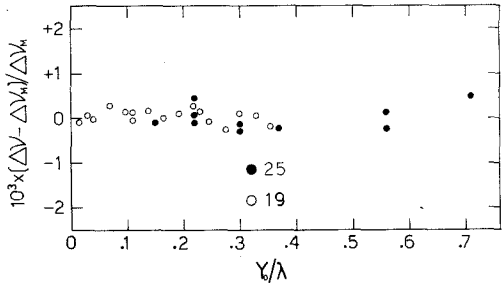

Fig. 6. The linewidth $\Delta\nu$ measured in He II. Open circles: $f_0 = 4556$ Hz, $T_\lambda - T = 0.5$ mK. Solid circles: $f_0 = 3056$ Hz, $T_\lambda - T = 0.9$ mK. The data are plotted as relative deviations from the mean and as a function of the ratio y_0/λ between vibration amplitude and viscous penetration depth.

amplitude, this error is temperature dependent and affects the final value of the critical exponent x. In our case, however, the driving voltage was kept so low that the vibration amplitude can slightly change without affecting the measurements.

3.1.4. Thermal Gradients

In the first experiments the main thermometer was placed at the bottom of the cell, while the wire was about 1 cm higher. With this setup the temperature of the liquid helium around the wire can be different from that measured by the main thermometer. Temperature gradients should be very small for $T < T_\lambda$, because of the high thermal conductivity of liquid He II, but they can be quite large for $T > T_\lambda$. As a clear example, we can quote our preliminary results in liquid He I.[9] Above the λ point the reduced viscosity was temperature independent up to $\varepsilon \simeq 10^{-4}$. The temperature around the wire was rather insensitive to the temperature changes near the main thermometer, indicating a temperature jump of about 200 μK. This strong gradient was due to the pumping action of the filling capillary, as explained in Section 2.2.

The behavior of the reduced viscosity changed drastically when the filling capillary was surrounded by a vacuum jacket, reaching the expected temperature dependence. To be sure, however, that the gradients have been reduced to small enough values, they must be measured. We performed the measurement as follows. The temperature T_{in} of the liquid helium (around the main thermometer) was kept constant to within ± 1 μK at about 30 μK above T_λ, and that of the main bath T_{out} was stabilized at various temperatures ranging 20–100 mK below T_λ. The power W needed to thermoregulate the cell, the resistance difference ΔR of the carbon resistors R_1 and R_2,

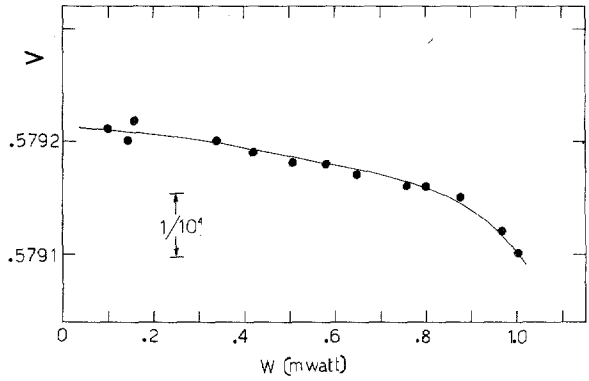

Fig. 7. Resonance signal v vs. thermoregulating power W at constant main thermometer resistance.

and the wire signal v_0 were all measured for every value of the temperature T_{out}. The results are shown in Figs. 7 and 8. Figure 7 shows that the signal decreases slowly as the thermoregulating power W increases. Remembering the temperature dependence of the wire signal (Fig. 5), we see that the temperature around the wire rises with respect to the main thermometer, as W increases. The thermal gradient can be easy calculated from the known

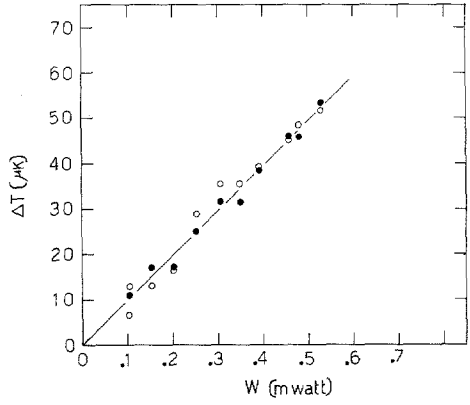

Fig. 8. The temperature difference ΔT between the wire region and the germanium region as a function of thermoregulating power W. Open circles: obtained from the change of the difference $R_2 - R_1$. Solid circles: obtained from wire signal measurements.

dependence of v_0 on T. The results are plotted in Fig. 8 together with values calculated from the resistance difference ΔR between R_1 and R_2. The results from both methods are in good agreement, and indicate a temperature difference of about 100 μK/mW).

Our working power was usually smaller than 0.1 mW, so that the systematic temperature error was always smaller than 10 μK. No detectable gradient was found below T_λ. In a second set of experiments we used a new cell, in which the main thermometer was placed at the wire level, to avoid gradient effects.

3.2. Measurements and Results

The measurements were performed in the following way. The helium was condensed in the cell, passing very slowly through the filtering apparatus. The temperature indicated by the germanium thermometer was stabilized to within ± 1 μK and the signal v_0 was monitored on a chart recorder. When the helium was clean, v_0 became constant very quickly. The linewidth was then measured at various amplitudes to exclude the presence of impurities, as explained in Section 3.1. If the result of the check was good, we started to measure. The viscosity was measured through the induced voltage v_0 as explained in Section 2.1. The ratio $v = V_{\text{out}}/V_D$ was measured with a differential voltmeter (Hewlett–Packard Model 3420 B), which can detect variations of about $1/10^5$. This voltmeter was balanced to zero and its output was continuously monitored by a chart recorder. The measurements were taken only after this output reached a stable level, usually 10–15 min after the stabilization of the germanium thermometer. This procedure assured the achievement of a good thermal equilibrium around the wire.

In a typical run we usually investigated both sides of the transition in about 8 h. At the end of each run the cell temperature was shifted to the initial value and the signal ratio v was remeasured. The reproducibility was good, a few parts in 10^5, indicating a good stability of the amplifiers.

The transition temperature T_λ measured with the germanium thermometer at the start and at the end of the run was reproducible to within ± 1 μK. The signal ratio and therefore the viscosity were found to be continuous through the transition. The spreading of the data at T_λ, observed in our first experiment as a possible viscosity jump, is therefore an instrumental effect, as suggested by us.[1] In that experiment the cell was in fact directly immersed in the main bath. Thermal stability above T_λ was not good enough, and the observed effect was probably due to erratic thermal gradients, or to a small increase in vibration amplitude induced by the boiling of the main bath.

3.3. Analysis of the Data

3.3.1. $\eta\rho$

As explained in Section 2.1, we measured the quantity $M = 1/f_0 v^2$, which is proportional to the product $\eta\rho$. From the graphical extrapolation of the data obtained very near the transition, we get the value $M_{\lambda 0}$ of M at T_λ (Fig. 5). Then we plot the values of the reduced quantity $M^* = |1-(M/M_{\lambda 0})|$ as a function of the reduced temperature $\varepsilon = (B/T_\lambda)|a_{\lambda 0} - a|$, using the measured value $a_{\lambda 0}$ that nulls the thermometer bridge at T_λ. If the plot is made on logarithmic scales, the data lie quite accurately on a straight line, indicating that we can fit them by the relation

$$M^* = Z\varepsilon^{\alpha} \tag{7}$$

We are interested in the behavior of M^* near the transition, where its values are small. To avoid having these data lose their real weight at small ε, we fit the data to the relation

$$\log M^* = \log Z + \alpha \log \varepsilon \tag{8}$$

The values of Z and α are first calculated minimizing the expression

$$\sum_{i=1}^{N} (\Delta\alpha_i)^2 = \sum_{i=1}^{N} \left(\alpha - \frac{\log M_i^* - \log Z}{\log \varepsilon_i}\right)^2 = (N-2)\sigma_\alpha^2 \tag{9}$$

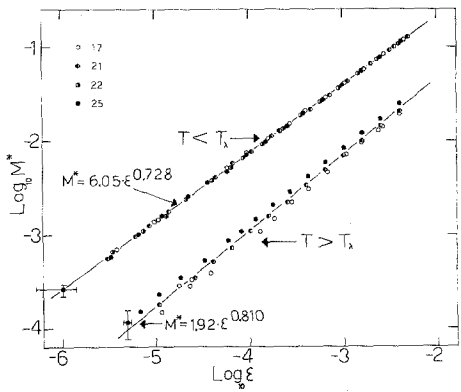

Fig. 9. Logarithm of the reduced quantity M^* as a function of the logarithm of the reduced temperature ε. The quantity M is proportional to the product $\eta\rho$. The straight lines represent the fitting functions. The data for $T > T_\lambda$ can be practically regarded as data for the viscosity η, because $\rho \simeq$ const in this region.

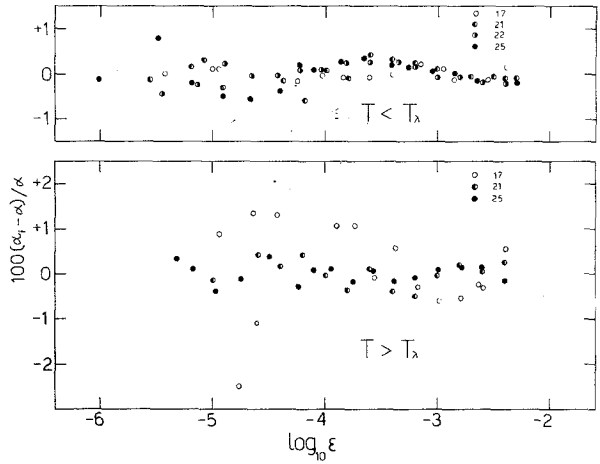

Fig. 10. Values of $\Delta\alpha_i/\alpha$ vs. $\log \varepsilon$, where $\Delta\alpha_i$ are the deviations defined in Section 3.3. The data are exactly the same as Fig. 9, but are plotted in a different way to show the quality of the fit.

The values α_0 and Z_0 obtained in this way depend obviously on the values $M_{\lambda 0}$ and $a_{\lambda 0}$ used in computing M_i^* and ε_i. Now, because $M_{\lambda 0}$ and $a_{\lambda 0}$ are affected by errors, we can change them, within their experimental errors, until we obtain the values that minimize the standard deviation σ_α. The best values for M_λ and a_λ for each run are calculated as follows. Below T_λ both α and Z are more sensitive to a_λ than to M_λ, because the signal v changes rapidly with temperature. Above T_λ, on the other hand, they are more sensitive to the choice of M_λ. Therefore we first use only the data for $T < T_\lambda$, and with $M_\lambda = M_{\lambda 0}$ we calculate σ_α for various values of a_λ. The value $a_{\lambda 1}$ that produces the minimum σ_α is our best value of a_λ at this step. In a second step we use only the data for $T > T_\lambda$, and with $a_\lambda = a_{\lambda 1}$ we calculate $M_{\lambda 1}$ in the same way. Then we repeat the calculation until the values for M_λ and a_λ converge to our final best values.

They converge very rapidly, and the corrections to $a_{\lambda 0}$ and $M_{\lambda 0}$ are rather small ones, well within the experimental errors of their measurements. The correction to $a_{\lambda 0}$, in particular, turns out to be very small for each run, as if the N values $|T_\lambda - T_i|$ were shifted by a constant ΔT that never exceeds 3 μK.

Our final results are shown in Fig. 9, and in a more sensitive plot in Fig. 10. From Fig. 9 we see that the points for $T < T_\lambda$ lie about one decade above those obtained at $T > T_\lambda$. For this reason the final result at $T < T_\lambda$ is better than that at $T > T_\lambda$. If we exclude very few points, we see that the power law (7) is followed below T_λ to within $\pm 0.5\%$ for each run over the full range

TABLE I

Final Results of Best-Fit Calculation for the Data Relative to the Product $\eta\rho$, the Quantity Directly Measured in the Experiment

Run number	α	Z
$T > T_\lambda$		
17	0.821 ± 0.008	1.84 ± 0.20
21	0.811 ± 0.003	1.87 ± 0.04
25	0.798 ± 0.002	2.04 ± 0.04
$T < T_\lambda$		
17	0.728 ± 0.001	6.18 ± 0.05
21	0.727 ± 0.002	6.05 ± 0.10
22	0.727 ± 0.002	5.92 ± 0.10
25	0.729 ± 0.003	6.04 ± 0.20

investigated. Above T_λ the deviation from the mean are within $\pm 1\%$ (Fig. 10). Table I reports the final data for the various runs. The errors quoted in the table are the standard deviations. The mean values are

$$\alpha = 0.810 \pm 0.012, \qquad Z = 1.92 \pm 0.10 \qquad \text{for} \quad T > T_\lambda$$

$$\alpha = 0.728 \pm 0.001, \qquad Z = 6.05 \pm 0.13 \qquad \text{for} \quad T < T_\lambda$$

3.3.2. The Viscosity η

$T > T_\lambda$. We are interested in the reduced viscosity $\eta^* = |1 - (\eta/\eta_\lambda)|$, rather than in the viscosity itself. From $\eta = H/\rho v^2 f = H(M/\rho)$, where H is

TABLE II

Results of Best-Fit Calculation for the Reduced Viscosity η^*[a]

Run number	x	A
$T > T_\lambda$		
17	0.822 ± 0.008	1.84 ± 0.16
21	0.812 ± 0.003	1.87 ± 0.05
25	0.798 ± 0.002	2.04 ± 0.04
$T < T_\lambda$		
17	0.817 ± 0.003	4.72 ± 0.08
21	0.821 ± 0.005	4.68 ± 0.20
22	0.842 ± 0.002	5.10 ± 0.07
25	0.830 ± 0.005	4.80 ± 0.24

[a]The results for $T > T_\lambda$ differ only weakly from the corresponding results of Table I, because $\rho \simeq$ const above T_λ.

temperature independent, we have $\eta^* = |1 - [(M/\rho)/(M/\rho)_\lambda]|$. Here M is the quantity we measure, while the density ρ is calculated using the interpolation formula by Kerr and Taylor.[10] The values M_λ and a_λ necessary for computing the reduced viscosity values η_i^* and the reduced temperatures ε_i are known from the best fit calculation of M^* explained before. The data are fitted by the relation

$$\eta^* = A\varepsilon^x \tag{10}$$

with the same best-fit procedure used for the product $(\eta\rho)^*$. The results of three runs are shown in Table II. The mean values are

$$x = 0.811 \pm 0.012 \qquad \text{and} \qquad A = 1.92 \pm 0.10$$

As ρ is almost constant in our temperature range above T_λ, $\eta^* \simeq (\eta\rho)^*$ and therefore $x \simeq \alpha$, $A \simeq Z$. Moreover, the plots of final results are practically the same as those shown in Figs. 9 and 10, and they are therefore omitted.

$T < T_\lambda$. Because relation (10) is a good description of the data above T_λ, we tried it for the data below T_λ also. To calculate η from the measured $\eta\rho_n$, we needed to know the normal density $\rho_n = \rho - \rho_s$. Experimental data for ρ_s are available only down to $\varepsilon \geq 2.5 \times 10^{-5}$. We analyzed our data for $\varepsilon > 2.5 \times 10^{-5}$ using the formula

$$\rho_s/\rho = 2.394\varepsilon^{0.6692}[1 + 0.6492\varepsilon^{0.5}) \tag{11}$$

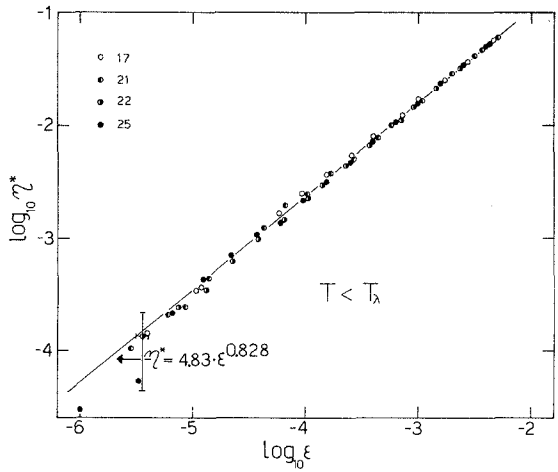

Fig. 11. Reduced viscosity vs. reduced temperature for $T < T_\lambda$. The straight line represents the power relation that fits the data for $\varepsilon \geq 2.5 \times 10^{-5}$.

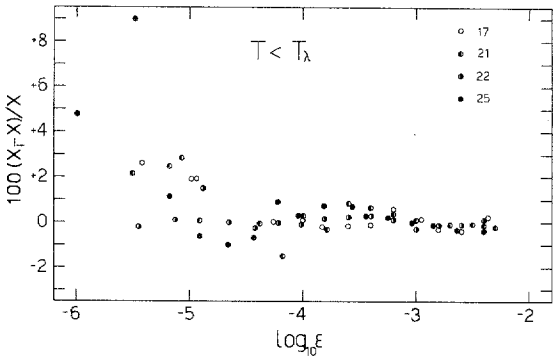

Fig. 12. The same data of Fig. 11 plotted as $\Delta x_i/x$ vs. $\log \varepsilon$. Small and systematic deviations from the fit are clearly apparent for $\varepsilon < 10^{-5}$.

proposed by Greywall and Ahlers[11] and we found that the data can be very well fitted by the simple law (10). The fit procedure is the same used for $T > T_\lambda$, and also the values M_λ and a_λ for each run are those known from the best fit calculation of M^*, the same used for $T > T_\lambda$. The results are shown in Table II and in Figs. 11 and 12. The mean values for x and A are

$$x = 0.828 \pm 0.013 \qquad \text{and} \qquad A = 4.83 \pm 0.21$$

4. DISCUSSION

If we insert in our plots for $T < T_\lambda$ the data in the range $\varepsilon < 2.5 \times 10^{-5}$, they show a small but systematic deviation from the power law (10). In this region, however, the data are given with a greater uncertainty. First of all, the normal density ρ_n needed to calculate η is a rapid function of T near the transition. A small error in the measured temperature produces a great error in ρ_n, and therefore in η. Second, the differences $\eta_\lambda - \eta_i$ to be measured in this region are smaller than $6 \times 10^{-4}\ \eta_\lambda$, and become comparable with their uncertainties. Therefore speculation about the viscosity behavior for $\varepsilon < 10^{-5}$ seems to be unwise. It is to be said, however, that the deviation of η^* from the power law (10) is of the same order and is systematic in all runs. If the power law (10), which describes the data very well at $T > T_\lambda$, is to be retained also for those at $T < T_\lambda$, two possibilities come to mind to explain the small and systematic deviation: (1) The interpolation formula (11) must be slightly corrected for $\varepsilon < 10^{-5}$ where ρ_s has not yet been measured. (2) There is a depression of the superfluid density near the surface of the wire. This depression has been suggested by various authors.* The superfluid

*For references see Eggington.[12]

density is thought to be zero in a layer of thickness d near the wall and to rise to the bulk value outside. The healing length d is temperature dependent, and is given by $d \simeq d_0 \varepsilon^{-2/3}$, with $d_0 \simeq 10^{-8}$ cm. It becomes comparable to our viscous penetration depth λ at $\varepsilon \simeq 10^{-5}$. The use of the bulk ρ_n in our calculations should therefore produce a strong deviation from the power law (10) at $\varepsilon \simeq 10^{-5}$, whereas we find only a weak deviation, as if the effect was not present. Nevertheless, the experiments on superflow in restricted geometries can be interpreted without introducing a superfluid healing length.[13] In our experiment we do not have a restricted geometry, even if the region that contributes to the viscous damping is a thin layer of liquid helium near the wire surface. If the interpretation of Pademore and Reppy is the correct one, then we should not get a changed ρ_n (or a ρ_s depression) near the wire. The normal density is altered only in restricted geometries. If, on the other hand, the healing length idea is correct, then we should have the ρ_s depression even if we do not work with a true restricted geometry. Because strong deviations from the power law (10) are absent in our results, we think that the point of view of Pademore and Reppy is the correct one. Measurements of ρ_n near a wall, if possible, would be highly desirable to settle the question.

If we neglect the weak deviation for $\varepsilon < 10^{-5}$ at $T < T_\lambda$, we realize that the critical exponents below and above T_λ are practically the same. If we apply in fact the correction discussed in Appendix A, we find

$$x = 0.811 \pm 0.012, \qquad A = 1.92 \pm 0.10 \qquad \text{for} \quad T > T_\lambda$$

$$x = 0.820 \pm 0.013, \qquad A = 4.66 \pm 0.21 \qquad \text{for} \quad T < T_\lambda$$

We can conclude that, within the experimental errors, the critical exponents are the same on both sides of the transition.

The only known measurements of viscosity comparable in precision with the present ones are those of Biskeborn and Guernsey.[7] The torsional frequency of their oscillating equipment (732 Hz) is comparable to our frequencies (3000, 4500 Hz). The maximum fluid velocity is 0.1–1 cm/sec in our experiment, 6×10^{-4} to 4×10^{-2} cm/sec in theirs. The main differences between the two experiments seem to be the following. The damping α_0 without helium amounts to 40% of the total damping for BG, while it is 0.25% in our case. We take measurements only when the liquid helium around the wire is in thermal equilibrium. The thermoregulation power (1×10^{-4} W) is essentially dissipated on the external bath, and therefore counterflow effects inside the cell should be absent. The procedure of BG is to record the data while warming the sample at various warming rates. No data were recorded while cooling. It can be calculated that a mean power of about 3×10^{-5} W ($\simeq 7 \times 10^{-7}$ W/cm^2) is needed to warm the sample liquid at

the mean warming rate used by BG. This heat flows directly through the first penetration depth of interest in the measurement.

Despite these differences, the results of the two experiments for $T > T_\lambda$ are in good agreement ($x = 0.80 \pm 0.05$ and $A = 2.1 \pm 0.9$ for the BG results). Below T_λ, however, the BG results show two regions. For $\varepsilon < 4 \times 10^{-4}$ they find a mean critical exponent $x = 0.65 \pm 0.03$, very different from our value $x = 0.820 \pm 0.013$. For $\varepsilon > 4 \times 10^{-4}$ their results approach the Ahlers power law fit[3] of the data from earlier experiments.[2] The results of the particular run shown in their Fig. 3 (the only data from the BG results in this region available to us) give $x = 0.80$ and $A = 5.0$ for $\varepsilon > 4 \times 10^{-4}$, in good agreement with our values. The discrepancy is therefore only in the region $\varepsilon < 4 \times 10^{-4}$, and only for $T < T_\lambda$. To remove it, we have performed every possible check that came to mind, looking for a possible systematic effect. The most relevant tests are reported throughout this paper. The results of the BG experiment are reported only in a letter, without the details necessary for a deeper comparison of the two experiments. The discrepancy is therefore essentially unexplained.

It is to be said, however, that for every physical quantity of interest, the critical region is usually well reached at $\varepsilon \simeq 10^{-2}$, and not so close to the transition as the results of BG seem to indicate ($\varepsilon \simeq 4 \times 10^{-4}$). The BG data for $\varepsilon > 4 \times 10^{-4}$ are therefore certainly representative of the critical region and are in fact in agreement with those of other authors.[2,3] The data for $\varepsilon < 4 \times 10^{-4}$ are probably affected by a weak systematic effect.

To conclude, we are confident that our final results, which have been presented in this paper, are correct, and that the values of the critical exponent are the same on both sides of the lambda transition.

APPENDIX A

The results of the measurements of the viscosity η can be described through the reduced viscosity η^* and the reduced temperature ε defined in Section 3 by the relationship

$$\eta^* = A\varepsilon^x \tag{A1}$$

The critical exponent x can be derived from a plot of $\log \eta^*$ as a function of $\log \varepsilon$. We are therefore interested in the systematic error in $\log \eta^*$. Let η be the "true" viscosity and η_1 the viscosity affected by some kind of approximation. They are connected by the relationship

$$\eta = \beta\eta_1 \tag{A2}$$

where β will be in general temperature dependent. If the error is small, we have

$$\Delta(\log \eta^*) = \log \eta_1^* - \log \eta^* \simeq \frac{\eta_1^* - \eta^*}{2.3\eta^*} = \frac{\Delta\eta^*}{2.3\eta^*} \tag{A3}$$

and

$$\Delta\eta^* = \frac{\eta}{\eta_\lambda} - \frac{\eta_1}{\eta_{1\lambda}} = \frac{\eta}{\eta_\lambda}\left(1 - \frac{\beta_\lambda}{\beta}\right) = (1-\eta^*)g(\varepsilon)$$

and finally

$$\Delta(\log \eta^*) \simeq \frac{1-\eta^*}{2.3\eta^*} g(\varepsilon) \simeq \frac{g(\varepsilon)}{2.3\eta^*} \tag{A4}$$

where $g(\varepsilon) = 1 - \beta_\lambda/\beta$. The relation (A4) also will be used in the following appendices.

We calculate now $g(\varepsilon)$ for the approximation of Section 2.1, using the relations[6]

$$\eta = (\pi a^2/2)(f\rho/m^2) \tag{A5}$$

$$k' = (\sqrt{2}/m) + (1/2m^2) \tag{A6}$$

$$k' = i_0 D/\rho v_0 f_0 \tag{A7}$$

where D is a constant. From (A5) and (A6) we get easily

$$\eta = \pi a^2 f \rho k'^2 / C(k') \tag{A8}$$

where $C(k') = 2 + k' + 2(1+k')^{1/2}$, and from (A7) and (A8)

$$\eta = \frac{1}{\rho f_0 v_0^2} \frac{\pi a^2 D^2 i_0^2}{C(k')} \tag{A9}$$

If the output voltage is $V_0 = G v_0$, and if $i_0 = V_D/R$, we get finally

$$\eta = \frac{H}{C(k')} \frac{1}{\rho f_0 v^2} = \frac{H}{C(k')} \eta_1 \tag{A10}$$

where v is the output/input ratio $v = V_0/V_D$ and H is constant when the magnetic field B, the driving resistance, and the gain G are kept constant. Our $g(\varepsilon)$ is therefore given by

$$g(\varepsilon) = 1 - \frac{C(k')}{C(k'_\lambda)} \tag{A11}$$

Expanding $C(k')$ to first order, we get

$$g(\varepsilon)\simeq(k'_\lambda-k')G(k'_\lambda) \tag{A12}$$

where $G(k'_\lambda)=[1+(1+k'_\lambda)^{1/2}](1+k'_\lambda)^{-1/2}C(k'_\lambda)^{-1}$.
From (A5) and (A6) we get easily

$$k'_\lambda-k'=(1/2)(n_\lambda^2-n^2)+\sqrt{2}(n_\lambda-n) \tag{A13}$$

where $n=(F\eta/\rho)^{1/2}$ and $F=2/\pi a^2 f$). In our temperature range F is assumed to be constant. Because of the small changes involved, we can take $(n_\lambda^2-n^2)\simeq 2n_\lambda(n_\lambda-n)$. Relation (A13) becomes

$$(k'_\lambda-k')\simeq(n_\lambda+\sqrt{2})F^{1/2}[(\eta_\lambda/\rho_\lambda)^{1/2}-(\eta/\rho)^{1/2}]=(n_\lambda+\sqrt{2})F^{1/2}P \tag{A14}$$

The factor P representing the square brackets can be rearranged as

$$P=\left(\frac{\eta_\lambda}{\rho_\lambda}\right)^{1/2}\frac{(1-\rho^*)^{1/2}-(1-\eta^*)^{1/2}}{(1-\rho^*)^{1/2}}$$

Expanding to the first term and neglecting ρ^* with respect to 1 in the denominator, we get

$$P\simeq(1/2)(\eta_\lambda/\rho_\lambda)^{1/2}(\eta^*-\rho^*) \tag{A15}$$

Combining (A15), (A14), (A12), and (A4), we have finally

$$\Delta(\log\eta^*)\simeq\frac{G(k'_\lambda)F^{1/2}(n_\lambda+\sqrt{2})}{4.6}\left(\frac{\eta_\lambda}{\rho_\lambda}\right)^{1/2}\left(\frac{1-\rho^*}{\eta^*}\right) \tag{A16}$$

With $a=2.5\times10^{-3}$ cm, $f=4000$ Hz, $\rho=0.146$ g/cm^3, $\eta_\lambda=27.5\times10^{-6}$ P, we get $G(k'_\lambda)=0.465$, $F^{1/2}=5.04$, $n_\lambda=6.9\times10^{-2}$, and finally

$$\Delta(\log\eta^*)\simeq 1.04\times10^{-2}(1-\rho^*/\eta^*) \tag{A17}$$

The temperature-independent term gives a constant error of about 1%. The straight line on the plot of $\log\eta^*$ vs. $\log\varepsilon$ is simply shifted by this term, leaving the exponent unaffected. The temperature-dependent term is proportional to ρ^*/η^*.

(a) $T>T_\lambda$. The density changes are much smaller than the viscosity changes. The ratio ρ^*/η^* is always smaller than 7×10^{-3}, and therefore $\Delta(\log\eta^*)$ is always smaller than 7×10^{-5}. The approximation $C(k')=$ const is quite good.

(b) $T<T_\lambda$. If $\rho_n^*=2.4\varepsilon^{0.666}$ and $\eta^*=4.83\varepsilon^{0.828}$, the temperature-dependent term is

$$\Delta(\log\eta^*)\simeq-5.2\times10^{-3}/\varepsilon^{0.162}$$

Its value is $E_a = -3.34\%$ for $\varepsilon_a = 1\times10^{-5}$ and $E_b = -1.10\%$ for $\varepsilon_b = 1\times10^{-2}$. From the definition (A3) it is easy to calculate the error in the exponent for the three decades of interest:

$$\frac{x_1 - x}{x} \simeq \frac{x_1 - x}{x_1} \simeq \frac{E_b - E_a}{(\log \varepsilon_b - \log \varepsilon_a)x_1} \simeq 0.9\%$$

APPENDIX B

Let v_0 be the output–input ratio in vacuum and v_1 that in liquid helium. Adding up dissipations, we have

$$1/v_1 = (1/v) + (1/v_0) \tag{B1}$$

v is the ratio that would be measured with a perfect wire ($Q_0 = \infty$). If now $\gamma = v/v_0 = Q/Q_0$, then

$$1/v_1 = (1/v)(1+\gamma) \tag{B2}$$

In our case $\gamma \simeq 2.5\times10^{-3}$, the effect of the wire dissipation is small, and it has been neglected. We calculate the error of this approximation. If η_1 is the approximate viscosity and η the true one, we have

$$\eta_1 = H/\rho f_0 v_1^2 = \eta(1+\gamma)^2 \simeq \eta(1+2\gamma) \tag{B3}$$

We use now the relations developed in Appendix A. In this case

$$g(\varepsilon) \simeq 1 - \frac{1+2\gamma}{1+2\gamma_\lambda} \simeq \frac{2(\gamma_\lambda - \gamma)}{1+2\gamma_\lambda} \simeq 2\gamma_\lambda \frac{\gamma_\lambda - \gamma}{\gamma_\lambda} \tag{B4}$$

The temperature dependence of Q_0 is very weak. We have found a relative change of 2×10^{-3} from $\varepsilon = 0$ to $\varepsilon = 10^{-2}$. Assuming v_0 and f_0 to be constant, we can write

$$\gamma = v/v_0 = [H^{1/2}/v_0(f_0\rho\eta)^{1/2}] \simeq (M/\rho\eta)^{1/2} \tag{B5}$$

where M is a constant. Now

$$(\gamma_\lambda - \gamma)/\gamma_\lambda \simeq 1 - (\rho_\lambda\eta_\lambda)^{1/2}/(\rho\eta)^{1/2} \simeq 1 - [(1-\rho^*)^{1/2}(1-\eta^*)^{1/2}]^{-1}$$

Expanding to first term, we find

$$(\gamma_\lambda - \gamma)/\gamma_\lambda \simeq -(1/2)(\eta^* + \rho^*)$$

Relation (A4) gives therefore

$$\Delta(\log \eta^*) \simeq \frac{g(\varepsilon)}{2.3\eta^*} \simeq \frac{\gamma_\lambda}{2.3\eta^*}\left(1 + \frac{\rho^*}{\eta^*}\right) \simeq -1.1\times10^{-3}\left(1 + \frac{\rho^*}{\eta^*}\right)$$

Our final result is similar to that of Appendix A. The temperature dependence is the same, but with a factor ten times smaller. The error in the critical exponent due to the approximation $Q_0 = \infty$ is therefore smaller than 0.1%.

APPENDIX C

We treat in this appendix the problem of the compound line. Let v and v' be the induced signal, at resonance, of the main and the second peak. Let l be the linewidth of the peaks and s the separation of their resonant frequencies f_0 and f_0'. As $l \simeq 10^{-3} f_0$ in our case, we use the approximation $f_0^2 - f^2 \simeq 2f(f_0 - f)$. The in-phase component v_F for the main peak can be written as

$$v_F = v \frac{l^2}{4(f_0 - f)^2 + l^2} \tag{C1}$$

and, with the position

$$f - f_0 = ul \tag{C2}$$

we have

$$v_F = v/(1 + 4u^2) \tag{C3}$$

and the out-of-phase component is

$$v_Q = -v[2u/(1 + 4u^2)] \tag{C4}$$

Similar relations hold for the second peak. We define now a separation factor S and an intensity factor R

$$S = s/l, \qquad R = v'/v \tag{C5}$$

With this position and adding up the contributions of both peaks we get for the components of the compound line

$$v_F = v\left(\frac{1}{1 + 4u^2} + \frac{R}{1 + 4(S - u)^2}\right) \tag{C6}$$

$$v_Q = -v\left(\frac{2u}{1 + 4u^2} - \frac{2R(S - u)}{1 + 4(S - u)^2}\right) \tag{C7}$$

In our technique the resonant compound frequency f_0 is given by the condition $v_Q = 0$. Therefore the number u_0 corresponding to f_0 is given from (C7) by

$$\frac{u_0}{1 + 4u_0^2} = \frac{R(S - u_0)}{1 + 4(S - u_0)^2} \tag{C8}$$

If R is small, the value of u_0 will be near the unperturbed value $u_0 = 0$. Moreover, in our case $s \simeq 10$ Hz, $l \simeq 3$ Hz, and $S \simeq 3$. Therefore

$$4u_0^2 \ll 1, \qquad u_0 \ll S, \qquad \text{and} \qquad 4S^2 \gg 1 \tag{C9}$$

With these approximations we have from (C8)

$$u_0 \simeq R/(4S) \tag{C10}$$

In the experiment we measure the component v_F at resonance. Its value can be obtained from (C6), (C9), and (C10):

$$v_1 \simeq v[1-4u_0^2+(R/4S^2)] \simeq v[1-(R^2/4S^2)+(R/4S^2)]$$

where v_1 is the value of the component v_F as perturbed by the second peak, and v is the unperturbed value. Rearranging the last relation between v and v_1, we obtain

$$1/v \simeq (1/v_1)[1+(R/4S^2)(1-R)] \simeq (1/v_1)[1+(R/4S^2)] \tag{C11}$$

If η_1 is the perturbed viscosity and η the true one, we have, from (B3), $\eta/\eta_1 = (v_1/v)^2$, and from (C11)

$$\eta = \eta_1[1+(R/4S^2)]^2 \simeq \eta_1[1+(R/2S^2)] = \eta_1\beta$$

The function $g(\varepsilon)$ of Appendix A is therefore, in the present case,

$$g(\varepsilon) \simeq (R/2S_\lambda^2)[(S_\lambda/S)^2-1] \tag{C12}$$

Using (A7) and the relation $1 \simeq \rho f_0 k'/\rho_F$ (Ref. 1, Section 2.1), we get finally

$$\begin{aligned} g(\varepsilon) &\simeq \frac{R}{2S_\lambda^2}\left(\frac{v_\lambda}{v}-1\right) \simeq \frac{R}{2S_\lambda^2}\left(\frac{\rho\eta}{\rho_\lambda\eta_\lambda}-1\right) \\ &\simeq \frac{R}{2S^2}[(1-\rho^*)(1-\eta^*)-1] \\ &\simeq -\frac{R}{2S^2}(\eta^*+\rho^*) \end{aligned} \tag{C13}$$

From Appendix A,

$$\Delta(\log \eta^*) \simeq -(R/4.6S_\lambda^2)[1+(\rho^*/\eta^*)]$$

which for $S_\lambda = 3$ becomes

$$\Delta(\log \eta^*) \simeq -2.4\times 10^{-2} R[1+(\rho^*/\eta^*)] \tag{C14}$$

which is similar to (A17). If $R = 0.1$, however, the factor $2.4\times 10^{-2}R$ is five times smaller than that of (A17), and the error in the critical exponent x is smaller than 2×10^{-3}. In our experiment the ratio R was usually about

5×10^{-2}, and therefore the error introduced by the second peak is quite negligible.

REFERENCES

1. L. Bruschi, G. Mazzi, M. Santini, and G. Torzo, *J. Low Temp. Phys.* **18**, 487 (1975).
2. R. D. Taylor and J. D. Dash, *Phys. Rev.* **106**, 398 (1957); D. F. Brewer and D. O. Edwards, *Proc. Roy. Soc. A* **251**, 247 (1959); B. Welber, *Phys. Rev.* **119**, 1816 (1960); J. T. Tough, W. D. McCormick, and J. G. Dash, *Phys. Rev.* **132**, 2373 (1963); R. W. H. Webeler and D. C. Hammer, *Phys. Lett*, **15**, 233 (1965); R. W. H. Webeler and G. Allen, *Phys. Lett.* **33A**, 213 1970).
3. G. Ahlers, *Phys. Lett.* **37A**, 151 (1971).
4. R. W. H. Webeler and G. Allen, *Phys. Rev. A* **5**, 1820 (1972).
5. J. T. Tough, W. D. McCormick, and J. G. Dash, *Phys. Rev.* **132**, 2373 (1963); *Rev. Sci. Instr.* **35**, 1345 (1964).
6. L. Bruschi and M. Santini, *Rev. Sci. Instr.* **46**, 1560 (1975).
7. R. Biskeborn and R. W. Guernsey, *Phys. Rev. Lett.* **34**, 455 (1975).
8. G. G. Stokes, *Mathematical and Physical Papers* (Cambridge University Press, London, 1922), Vol. III, p. 38.
9. L. Bruschi, G. Mazzi, M. Santini, and G. Torzo, in *Proc. of the 14th Int. Conf. on Low Temp. Phys.* (North-Holland, Amsterdam, 1975).
10. E. G. Kerr and R. D. Taylor, *Ann. Phys.* **26**, 292 (1964).
11. D. S. Greywall and G. Ahlers, *Phys. Rev. A* **7**, 2145 (1973).
12. A. Eggington, in *The Helium Liquids*, J. G. M. Armitage and I. E. Farquhar, eds. (Academic Press, London, 1975).
13. T. C. Pademore and J. D. Reppy, *Phys. Rev. Lett.* **33**, 1410 (1974).